



# Influence of ambient conditions and water flow on the performance of pre-cooled natural draft dry cooling towers

Suoying He<sup>\*</sup>, Zhiqiang Guan, Hal Gurgenci, Ingo Jahn, Yuanshen Lu, Abdullah M. Alkhedhair

Queensland Geothermal Energy Centre of Excellence, School of Mechanical and Mining Engineering, The University of Queensland, QLD 4072, Australia

## Abstract

A simplified heat and mass transfer model in cellulose medium was developed to predict the air outlet temperature and humidity after evaporative cooling. The model was used to simulate the operation of pre-cooled Natural Draft Dry Cooling Towers (NDDCTs) by a validated MATLAB code. The effects of supplied water flow rate to the media, ambient temperature and humidity on the performance of pre-cooled NDDCTs were investigated. It was found that the effect of the selected water flow rates on tower performance is negligible. Both ambient temperature and humidity affect the tower performance.

**Keywords:** Natural draft dry cooling tower; cellulose medium; heat rejection; pressure drop

## Nomenclature

$A$	Area, $m^2$	$\theta_m$	The mean flow incidence angle, $^\circ$
$A_{e3}$	Effective reduced flow area, $m^2$	$k$	Thermal conductivity, $W/(m\ K)$
$A_s$	Heat and mass transfer area, $m^2$	$\mu$	Dynamic viscosity, $kg/(m\ s)$
$c_p$	Specific heat, $J/(kg\ K)$	$\nu$	Kinetic viscosity, $m^2/s$
$d$	Diameter, $m$	$\xi$	Specific surface area of medium, $m^2/m^3$
$F_T$	Temperature correction factor	$\rho$	Density, $kg/m^3$
$f_D$	Friction factor inside the tube	$\sigma$	Ratio of minimum to free stream flow area
$g$	Gravitational acceleration, $m/s^2$	$\sigma_c$	Contraction ratio
$H$	Height, $m$	$\phi_{cf}$	Dimensionless mean temperature difference
$h$	Heat transfer coefficient, $W/(m^2\ K)$ ; Enthalpy, $J/kg$	$\phi_h, \phi_c$	Dimensionless temperature changes of water and air
$h_{ae}$	Effective heat transfer coefficient, $W/(m^2\ K)$		
$h_{wb2}$	Enthalpy of saturated water vapour at wet-bulb temperature of the inlet air, $J/kg$		
$K$	Loss coefficient	<b>Subscripts</b>	
$l$	Medium thickness, $m$	1	The conditions at ground level
$le$	Characteristic length, $le = V / A_s = \xi^{-1}$ , $m$	2	The conditions at the average height of tower inlet; inlet or before pre-cooling
$m$	Mass flow rate, $kg/s$	3	The conditions at the entrance of heat exchanger; outlet or after pre-cooling
$\Delta p$	Pressure drop, $Pa$	4	The conditions at the exit of heat exchanger
$Q$	Heat transfer rate, $W$	5	The conditions at the outlet of the tower
$Q_1, Q_2$	Heat rejection rate, $W$	$a$	Air or based on air side; air dry bulb
$Q_w$	Water flow rate, $m^3/h$	$ci$	Inlet contraction
$RH$	Air relative humidity, %	$ct$	Separation and redirection of flow at the lower edge of tower shell
$T$	Temperature, $K$	$ctc$	Contraction at heat exchanger
$\Delta T$	Temperature difference, $K$	$cte$	Expansion at heat exchanger
$u$	Velocity, $m/s$	$d$	Downstream
$1 / (UA)$	Overall thermal resistance, $K/W$	$e$	Evaporation; tube
$V$	Volume of medium, $m^3$	$f$	Fin
$W$	Medium width, $m$	$fr$	Total effective front of heat exchanger
$w$	Humidity ratio, $kg_w/kg_a$	$he$	Form and friction at heat exchanger
		$hes$	Heat exchanger supports
		$hx$	Heat exchanger
<b>Non-dimensional Groups</b>		$lm1, lm2$	Logarithmic mean
$Fr_D$	Densimetric Froude number defined in text	$LVO$	Latent heat of vaporization evaluated at $0^\circ C$
$Nu$	Nusselt number, $Nu = (h\ le) / k$	medium	Cellulose medium

\* Corresponding author. Tel/Fax: +61-7-3365-1268; E-mail: uqshe1@uq.edu.au (S. He)

$Nu_w$	Nusselt number of water, $Nu_w = (h_w d_e) / k_w$	<i>mfr</i>	Medium front
$Ny$	Characteristic heat transfer parameter, $m^{-1}$	<i>s</i>	Sensible
$Pr$	Prandtl number, $Pr = \nu / \alpha = (\mu c_p) / k$	<i>to</i>	Kinetic energy at the outlet of tower;
$Re$	Reynolds number, $Re = (u_a l_e) / \nu$	<i>ts</i>	Tower supports
$Re_w$	Reynolds number of water, $Re_w = (\rho_w u_w d_e) / \mu_w$	<i>v</i>	Saturated water vapour
$Ry$	Characteristic flow parameter, $m^{-1}$	<i>w</i>	Water or based on water side
<b>Greek Symbols</b>		<i>wb</i>	Wet bulb
$\alpha$	Thermal diffusivity, $m^2/s$	<i>wi, wo</i>	Hot water inlet and outlet
$\eta$	Cooling efficiency, %		
$\eta_{lb}$	Correction factor		

## 1. Introduction

A Natural Draft Dry Cooling Tower (NDDCT) creates the air flow through the heat exchanger bundles by means of buoyancy effects due to the difference in air density between the inside and outside of the tower [1]. NDDCTs have received widespread attention because they do not consume water, have low maintenance requirements and cause small parasitic losses. Since NDDCTs rely mainly on convective heat transfer to reject heat from the working fluid, they are not as effective as wet cooling towers which can achieve much higher rates of cooling by water evaporation [2]. The performance of dry cooling is particularly reduced when the ambient air temperature is high. Reduced cooling tower performance lowers the efficiency of the thermal power stations they are serving. Hybrid cooling may be a cost-effective solution by limiting water consumption only to the periods when the ambient temperatures are too high [3-5]. Hybrid cooling is the combination of dry and wet cooling. Kroger [3] reported that there are many ways of combining dry and wet cooling, including deluge enhancement, combinations of dry and wet cooling units, pre-cooling the entering air by humidification. Rising energy costs, together with water scarcity, urge the use of evaporative cooling systems that are economical and highly water and energy efficient [6, 7].

Past research has focussed on hybrid cooling with mechanical draft cooling towers. An earlier paper [8] by the present authors is the first report of a study investigating the conditions under which wetted-medium evaporative cooling can be used in NDDCTs. The present paper expands that study by incorporating the effect of water flow rate through wetted media as well as the effect of ambient temperature and relative humidity on the cooling performance of NDDCTs.

The objectives of this paper are threefold: (1) to develop a model to predict air outlet temperature and humidity after evaporative cooling and the water evaporation rate; (2) to determine the effects of water flow rate through the medium and ambient conditions on the pre-cooled NDDCT performance; (3) to investigate the water evaporation of the wetted-medium evaporative pre-cooling systems. A simplified heat and mass transfer model in wetted media was developed to predict the air outlet temperature and humidity after evaporative cooling. The model was used to simulate the effects of pre-cooling systems on the NDDCT performance. The trade-off between cooling performance and pressure drop was included. The MATLAB code of NDDCT without pre-cooling system was compared with the case study reported by Kroger [1] and found good agreement. This validated MATLAB code was then adapted to simulate the operation of the proposed tower with and without pre-cooling.

## 2. Configurations of Pre-cooled NDDCT

### 2.1 Pre-cooled NDDCT

A hyperbolic, natural-draft, dry-cooling tower pre-cooled with wetted medium packing is shown in Fig. 1, including the cross section, top view of the cooling tower and partial magnification of pre-cooling system. The wetted media considered in this study is made of cellulose paper as can be found in commercial brand, CELdek evaporative cooling pad. The media will be referred to as cellulose media in the rest of the paper. The heat exchangers used extruded bimetallic finned tubes. The heat exchanger bundles were laid out horizontally at the lower end of the tower and were arranged in the form of A-frames placed in a radial pattern. The density of the heated air inside tower was less than the density of the atmosphere outside the tower. Therefore, the pressure inside the tower was less than the external pressure at the same elevation, which led to the air flowing through the tower at a rate constrained by the various flow resistances encountered, the cooling tower dimensions, and the heat exchanger characteristics [1].

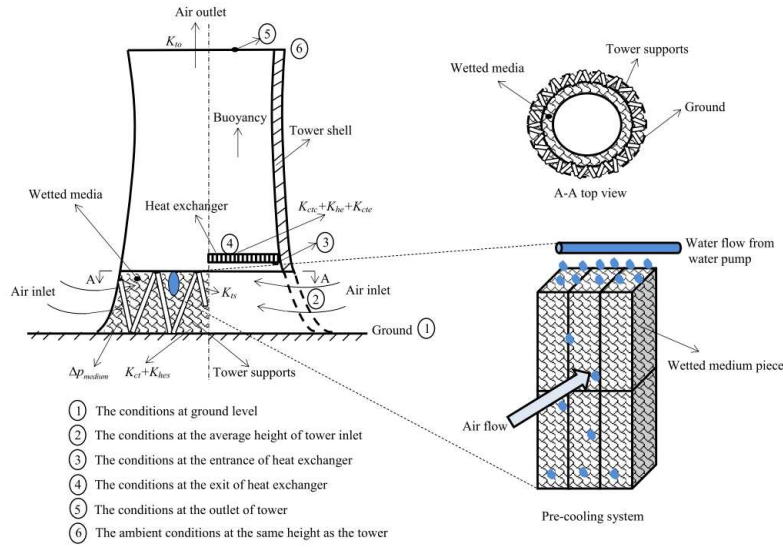


Fig. 1. NDDCT pre-cooled with cellulose media (not to scale)

In this configuration, the entire cylindrical shell inlet area of the tower was covered with one layer of 100mm thick cellulose media. To cover the entire tower inlet area of 3091 m<sup>2</sup> with cellulose piece dimensions of 2.0m height, 0.6m width and 0.1m thickness, 2639 cellulose pieces were put side by side to form a cylindrical shell around the tower inlet and piled up to meet the height of the tower inlet (see Fig. 1). The media are easy to cut to fit the corresponding shape. The cost of media is estimated to be around \$180,000 in 2012 Australian Dollars [9].

Water was distributed over the top of the media by distributor and dripped down by gravity and capillarity to wet the media uniformly. Excess water was collected at the bottom of the media and recirculated by pump. Air passed through cellulose media to form a cross-flow heat and mass exchange process. The water deposited on the media evaporated by extracting its evaporation heat from the air stream and thus cooled the air. The pre-cooled air then flowed through the heat exchanger bundles to cool the tube-side fluid coming from thermal power plant. The tower considered in this study has a height of 120m, a representative height for NDDCTs used in thermal power plants. The details of the tower and heat exchanger are summarised in Table 1.

Table 1 Specifications of the cooling tower and heat exchanger

Heat exchanger specifications	Cooling tower specifications
Hydraulic diameter of tube, $d_e=0.0216$ m	Tower height, $H_5=120$ m
Fin diameter, $d_f=0.0572$ m	Tower inlet height, $H_3=13.67$ m
Effective length of finned tube, $L_{te}=14.4$ m	Heat exchanger exit height, $H_4=15.54$ m
Number of tube rows, $n_r=4$	Tower inlet diameter, $d_3=83$ m
Number of tubes per bundle, $n_{tb}=154$	Tower outlet diameter, $d_5=58$ m
Number of water passes, $n_{wp}=2$	Number of tower supports, $n_{ts}=60$
Number of bundles, $n_b=142$	Length of tower support, $L_{ts}=15.78$ m
Apex angle of A-frame, $\theta=61.5^\circ/2$	Diameter of tower support, $d_{ts}=0.5$ m
Inside area of tube per unit length, $A_{ti}=0.0679$ m <sup>2</sup> /m	
Inside cross-sectional flow area, $A_{ts}=3.664 \times 10^{-4}$ m <sup>2</sup>	
Total effective frontal area of bundles, $A_f=4444.6$ m <sup>2</sup>	

The design conditions of the proposed tower without pre-cooling are given in Table 2.

Table 2 Design conditions of the proposed tower without pre-cooling

Items	Values and units
The atmospheric pressure, $P_{a1}$	101.325 kPa
Ambient air temperature, $T_{a1}=T_{a2}$	293.15 K (20 °C)
Ambient air relative humidity, $RH_1=RH_2$	30 %
Air mass flow rate, $m_a$	10912 kg/s
Air temperature exit heat exchanger, $T_{a4}$	319.75 K (46.6 °C)
Hot water mass flow rate, $m_w$	4390 kg/s
Hot water inlet temperature, $T_{wi}$	333.15 K (60 °C)
Hot water outlet temperature, $T_{wo}$	317.05 K (43.9 °C)
Heat rejection rate, $Q_1=Q_2$	296 MW

## 2.2. Cellulose Media

Wetted-medium evaporative cooling is presently applied in many fields and shows good cooling performance. Applications include evaporative coolers and cooling ventilation systems [10, 11], greenhouse cooling [6], warehouse cooling and product storage [12, 13], nursery cooling [14], poultry, hog and livestock cooling [15, 16], wet cooling towers in thermal power plants [3], and inlet air cooling of gas turbines [17]. The above applications are proved to be effective although the pressure drop introduced by wetted media causes some parasitic losses. While pre-cooling the inlet air of NDDCT, however, the additional pressure drop will have a strong effect on the air flowing through the tower and therefore may significantly impair tower heat rejection. There is a trade-off between cooling performance and pressure drop.

It is widely acknowledged that medium is the most important element in wetted-medium cooling systems [6, 12, 18]. Wetted media fulfil two main functions. Firstly, they provide a large contact surface for heat and mass exchange between water and air flows. Secondly, they delay the fall of water, ensuring that the exchange process lasts longer [6, 19, 20]. Cellulose medium is a high efficiency evaporative cooling medium that is engineered to provide maximum cooling, low pressure drop and long life of reliable service [21]. The low pressure drop is of critical importance to NDDCT operation. Usually, the cooling efficiency of cellulose media varies from 70% to over 95%, depending on medium thickness and air velocity [22]. The longevity of cellulose media can be even more than 10 years with proper maintenance [21-23]. To this end, a type of cellulose medium was used in this study.

## 3. Numerical Simulation

In section 3.1.1, a simplified heat and mass transfer model in wetted media was developed to predict the air outlet temperature and humidity after evaporative cooling, and the water evaporation rate. This model was used to develop a pre-cooled NDDCT model in section 3.1.2 with considering the trade-off between cooling performance and pressure drop. A MATLAB code was developed in section 3.2 to simulate the operation of the proposed tower with and without pre-cooling.

### 3.1 Mathematical Models

#### 3.1.1 Cellulose Medium Model

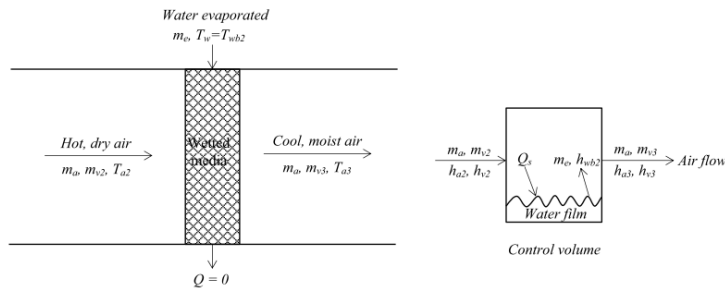


Fig. 2. Transfer process of evaporative cooling system and a control volume

Heat and mass transfer coefficients and the pressure drop are the main characteristics of cellulose medium for the purpose of the present application. The heat and mass transfer processes in the wetted-medium evaporative cooling system and a control volume are demonstrated in Fig. 3. It was assumed that the medium was wetted uniformly and fully; the transfer area for heat and mass transfer was identical; both dry air and water vapour could be treated as ideal gases; the thermal properties of air and water were constant; the heat transfer from surroundings  $Q$  was negligible; the recirculating water temperature  $T_w$  was equal to the wet-bulb temperature of the incoming air  $T_{wb2}$ . Then, the mass balance of the mixture of dry air and water vapour or the rate of water evaporation is given by,

$$m_e = m_{v3} - m_{v2} = m_a (w_{a3} - w_{a2}) \quad (1)$$

and the energy balance is

$$(m_a h_{a3} + m_{v3} h_{v3}) - (m_a h_{a2} + m_{v2} h_{v2}) = m_e h_{wb2} - Q_s \quad (2)$$

Theoretically, evaporative cooling is adiabatic cooling, the air dry-bulb temperature is decreased because it gives up sensible heat, and the water vapour becomes part of the air and carries the latent heat with it [10]. In

Eq.(2),  $Q_s$  is the sensible heat given up by the air and  $m_e h_{wb2}$  is the heat carried by the evaporated water (including the latent heat of water vaporization and the energy of liquid water).

Table 3 Main equations used in the deduction of air outlet temperature

Condition descriptions	Equations	Equation numbers
Ideal gas assumption and substituting Eq.(1) into Eq.(2)	$Q_s = m_a c_{pa} (T_{a2} - T_{a3}) + m_a [w_{a2} (h_{v2} - h_{wb2}) - w_{a3} (h_{v3} - h_{wb2})]$	(3)
Ignore the small changes in specific heat of water vapour	$Q_s = m_a c_{pa} (T_{a2} - T_{a3}) + m_a c_{pv} [w_{a2} (T_{a2} - T_{wb2}) - w_{a3} (T_{a3} - T_{wb2})]$ , $h_v = c_{pv} T_a + h_{LV0}$	(4)
Humidity ratio is far less than one	$Q_s = m_a c_{pa} (T_{a2} - T_{a3})$	(5)
Employing log mean temperature difference	$Q_s = h A_s \Delta T_{lm1}$ , $\Delta T_{lm1} = (T_{a3} - T_{a2}) / [\ln((T_{a3} - T_{wb2}) / (T_{a2} - T_{wb2}))]$ , $A_s = \xi V = \xi A_{mfr} l$ , $m_a = \rho_a u_a A_{mfr}$ , $A_{mfr} = W \times H$	(6)

Considering the equations in Table 3, the air outlet temperature can be expressed as,

$$T_{a3} = T_{wb2} + (T_{a2} - T_{wb2}) \exp\left(\frac{-h \xi l}{\rho_a u_a c_{pa}}\right) \quad (7)$$

Similar form of air outlet dry-bulb temperature was obtained and validated by J.M. Wu [24]. This study employed Eq.(7) to predict the air outlet dry-bulb temperature. The air outlet humidity was determined from air outlet dry-bulb temperature and wet-bulb temperature (wet-bulb temperature kept constant during adiabatic cooling), and then the water evaporation rate was calculated from Eq.(1). To predict the air outlet temperature after cooling using Eq.(7), one needs to know the heat transfer coefficient of the studied media. A. Franco [6] did experimental study of different types of cellulose media in various conditions to develop correlations for heat and mass transfer coefficients and pressure drop, and gave the heat transfer coefficient by means of least square fitting as,

$$Nu = 0.172 \left(\frac{le}{l}\right)^{0.32} Re^{0.85} Pr^{1/3}, R^2 = 0.991 \quad (8)$$

The properties in Eq.(8) are those of dry air at the average dry-bulb temperature through wetted media. The definitions of non-dimensional groups are given in Nomenclature. The characteristic length in non-dimensional groups is  $le = V / A_s = \xi^{-1}$ . The air velocity is  $u_a = m_a / (\rho_a A_{mfr})$ .

The pressure drop introduced by wetted medium is also of critical importance in NDDCT applications. It is critical because the pressure drop will affect air flow passing through the tower. In this study, the pressure drop was represented by the experimental correlation developed by A. Franco [6].

$$\Delta p_{medium} = 0.768 \left(\frac{le}{l}\right)^{-0.469} (1 + Q_w^{1.139}) u_a^2, R^2 = 0.987 \quad (9)$$

The medium geometry was represented by the non-dimensional length,  $le / l$ . A. Franco [6] reported that Eq.(9) was adequate to represent different medium geometries, and a correct value for the non-dimensional length was used. The characteristics of cellulose medium selected for this study are summarized in Table 4. The 60 degree flute carries water to the air inlet side while the 30 degree flute is aligned with the direction of air flow.

Table 4 Characteristics of cellulose medium

Medium type	Medium thickness	Angles	Flute height	Specific surface area
Cellulose media	$l=100$ mm	$60^\circ$ - $30^\circ$	7.5 mm	$\xi = 361.516$ m <sup>2</sup> /m <sup>3</sup> [6]

The cooling efficiency is generally considered as the key factor in determining the performance of direct evaporative cooling systems. It represents how close the exiting air gets to the state of saturation [22]. The definition of cooling efficiency was given by J.R. Watt [10] as,

$$\eta = \frac{T_{a2} - T_{a3}}{T_{a2} - T_{wb2}} \times 100\% \quad (10)$$

### 3.1.2 Pre-cooled NDDCT Model

#### (1) Thermal Analysis

In this section, the heat transfer in the heat exchanger of the proposed NDDCT is analysed. The heat exchanger geometry is already described in Table 1. The main equations and correlations are listed in Table 5.

In Table 5,  $Q_1 = Q_2$  states that the heat transferred into the air equals to the heat extracted from the water and this heat is transferred through the heat exchanger. The heat exchanger inlet air temperature,  $T_{a3}$ , can be calculated by Eq.(7) combined with Eq.(8). The air conditions at the elevation 2 are the atmospheric conditions.  $a_{i,k}$  in the expression of  $F_T$  are the sixteen values of the empirical constant for crossflow with four tube rows and two tube passes, which can be found in reference [3] based on the heat exchanger geometry in Table 1. In Eq.(14), the other thermal resistances like the resistances due to the tube wall, fouling, and the thermal contact resistance between the tube and the fin are ignored. The effectiveness of finned surface is  $e_f = 1 - A_f(1 - \eta_f) / A_a$ . Schmidt and Zeller's empirical method to determine the fin efficiency  $\eta_f$  for a radial fin of uniform thickness as recommended by Kroger [3] was used in this study. In Eq.(18), all the thermophysical properties are evaluated at the bulk mean temperature of water. The friction factor  $f_D$  inside the tube was calculated according to Haaland's correlation [25].

Table 5 Main correlations used in thermal analysis

Descriptions	Equations, correlations, conditions and references	Equation numbers
Energy equations	$Q_1 = m_a c_{pa} (T_{a4} - T_{a3}) = m_w c_{pw} (T_{wi} - T_{wo})$	(11)
	$Q_2 = (UA F_T [(T_{wi} - T_{a4}) - (T_{wo} - T_{a3})]) / (\ln[(T_{wi} - T_{a4}) / (T_{wo} - T_{a3})]) = UA F_T \Delta T_{lm2}$	(12)
Temperature correction factor	$F_T = 1 - \sum_{i=1}^4 \sum_{k=1}^4 a_{i,k} (1 - \varphi_{cf})^k \sin(2i \arctan(\varphi_h / \varphi_c))$ , $\varphi_h = (T_{wi} - T_{wo}) / (T_{wi} - T_{a3})$ , $\varphi_c = (T_{a4} - T_{a3}) / (T_{wi} - T_{a3})$ , $\varphi_{cf} = (\varphi_h - \varphi_c) / (\ln[(1 - \varphi_c) / (1 - \varphi_h)])$ , Roetzel [26]	(13)
Overall thermal resistance	$1 / (UA) = 1 / (h_{ae} f A_a) + 1 / (h_w A_w)$	(14)
Effective air-side heat transfer coefficient $h_{ae}$	$h_{ae} A_a = h_a e_f A_a = ((F_T \Delta T_{lm2}) / Q_2 - 1 / (h_w A_w))^{-1}$	(15)
Characteristic heat transfer parameter $Ny$	$\eta_{tb} Ny = h_{ae} A_a / (k_{a34} A_{fr} Pr_{a34}^{0.333})$ , $\eta_{tb} = n_{tb-actual} / n_{tb-maximum}$ , Kroger [3]	(16)
	$Ny = 383.617313 R_y^{0.523761}$ , $R_y = m_a / (\mu_{a34} A_{fr})$ , Kroger [3]	(17)
Water-side heat transfer	$Nu_w = ((f_D / 8) (Re_w - 1000) Pr_w [1 + (d_e / L_{te})^{0.67}]) / (1 + 12.7 (f_D / 8)^{0.5} (Pr_w^{0.67} - 1))$ $2300 < Re_w < 10^6$ , $0.5 < Pr_w < 10^4$ , and $0 < d_e / L_{te} < 1$ , Gnielinski [27]	(18)

#### (2) Pressure Drop Analysis

In this section, the pressure drop of the pre-cooled NDDCT is analysed. The main equations and correlations are listed in Table 6.

In Table 6, the draft equation balances the buoyancy forces against the total pressure drop (or the sum of flow resistances) across various components of the tower (see Eq.(19)). The flow resistances include the pressure drop across the wetted medium  $\Delta p_{medium}$ ; loss at tower supports  $\Delta p_{ts}$  (Since cellulose media are arranged in the form of a cylindrical shell around the tower inlet, this loss is already accounted for by the pressure drop across cellulose media); loss due to the separation and redirection of flow at the lower edge of tower shell  $\Delta p_{ct}$ ; loss at heat exchanger supports  $\Delta p_{hes}$ , this loss is generally negligible; contraction loss  $\Delta p_{ctc}$ , the frictional loss of heat exchanger  $\Delta p_{he}$ , and expansion loss at heat exchanger  $\Delta p_{cte}$ ; the flow is essentially isentropic from 4 to 5 with a further loss  $\Delta p_{t0}$  in kinetic energy at the outlet of tower. In Eq.(21), the subscript  $hx$  represents

that the corresponding loss coefficients are referred to the frontal area of heat exchanger and the mean density of air flowing through it. The major components of the total flow resistance are the pressure drop across wetted medium and the frictional loss due to the heat exchanger. The pressure drop across wetted medium  $\Delta p_{medium}$ , was calculated by the correlation developed by A. Franco (Eq.(9)). In Eq.(23) and Eq.(24), the effective reduced flow area at tower inlet cross section is  $A_{e3} = A_{fr} \sin \theta$ . The contraction ratio  $\sigma_c$  in Eq.(23) was determined according to Rouse's correlation [28].

Table 6 Main correlations used in pressure drop analysis

Descriptions	Equations, correlations, conditions and references	Equation numbers
	$\Delta p_{total} \approx (\rho_{a1} - \rho_{a4})g [H_5 - (H_4 + H_3) / 2] = \Sigma \text{ flow resistances}$	(19)
Draft equations	$\Delta p_{total} = \Delta p_{medium} + \Delta p_{ct} + \Delta p_{ctc} + \Delta p_{he} + \Delta p_{cte} + \Delta p_{to}$	(20)
	$\Delta p_{total} = \Delta p_{medium} + (K_{ct} + K_{ctc} + K_{he} + K_{cte})_{hx} (m_a / A_{fr})^2 / (2\rho_{a34}) + K_{to} (m_a / A_5)^2 / (2\rho_{a5})$	(21)
Tower inlet loss coefficient	$K_{ct} = \left[ 0.072(d_3/H_3)^2 - 0.34(d_3/H_3) + 1.7 \right] (\rho_{a34}/\rho_{a3}) (A_{fr}/A_3)^2$	(22)
Contraction loss coefficient	$K_{ctc} = (1 - 2/\sigma_c + 1/\sigma_c^2) (\rho_{a34}/\rho_{a3}) (A_{fr}/A_{e3})^2$	(23)
Expansion loss coefficient	$K_{cte} = (1 - A_{e3}/A_3) (\rho_{a34}/\rho_{a4}) (A_{fr}/A_{e3})^2$	(24)
Heat exchanger loss coefficient	$K_{he} = \left[ (1383.94795/Ry)^{0.332458} + (2/\sigma^2) ((\rho_{a3}-\rho_{a4})/(\rho_{a3}+\rho_{a4})) \right] + (2\rho_{a4}(1/\sin\theta_m - 1) / (\rho_{a3}+\rho_{a4})) \left[ ((1/\sin\theta_m) - 1) + 2K_{ci}^{0.5} \right] + (2\rho_{a3}K_d) / (\rho_{a3}+\rho_{a4})$	(25)
	$Ry = m_a / (\mu_{a34} A_{fr}), \theta_m = 0.0019\theta^2 + 0.9133\theta - 3.1558$	
	$K_d = \exp(5.488405 - 0.2131209\theta + 3.533265 \times 10^{-3} \theta^2 - 0.2901016 \times 10^{-4} \theta^3), \text{ Kroger [1, 3]}$	
	$K_{to} = -0.28Fr_D^{-1} + 0.04Fr_D^{-1.5}$	
Tower outlet loss coefficient	$Fr_D = (m_a / A_5)^2 / [\rho_{a5}(\rho_{a6}-\rho_{a5})gd_5], 0.5 \leq d_5 / d_3 \leq 0.85$	(26)
	$5 \leq \left[ (1383.94795/Ry)^{0.332458} + (2/\sigma^2) ((\rho_{a3}-\rho_{a4})/(\rho_{a3}+\rho_{a4})) \right] \leq 40$	

### 3.2 Numerical Method

The values of air mass flow rate, heat transfer coefficient and pressure drop of cellulose media, heat rejection rate and water evaporation rate can be found when the energy and draft equations are satisfied. A MATLAB code was developed to find these values by an iterative process. The fixed variables during iteration were tower specifications and heat exchanger specifications, hot water flow rate, hot water inlet temperature, medium type and thickness. The iteration variables were air temperature exit the heat exchanger and cooling efficiency. The iteration procedure is summarised as follows.

Step 1, a preliminary air mass flow rate  $m_{a0}$  was estimated. It was assumed that the tower was without cellulose pre-cooling, and that the air leaving the heat exchanger was at a temperature equal to the hot water inlet temperature. By neglecting all flow resistances other than the losses due to the heat exchanger bundles, a preliminary air mass flow rate  $m_{a0}$  passing through the tower could be obtained.

Step 2, calculating a new air mass flow rate  $m_{a1}$  used more rigorous draft equation. This time, all the losses were considered including the pressure drop across cellulose media. After solving the draft equation, a new value of air mass flow rate  $m_{a1}$  would be found.

Step 3, calculation of wetted-medium evaporative cooling used the new air mass flow rate  $m_{a1}$ . Since the properties in Eq.(8) are those of dry air at the average dry-bulb temperature through cellulose media, an initial cooling efficiency defined by Eq.(10) was set as zero. The air dry-bulb temperature after cooling was calculated according to Eq.(10), and the average dry-bulb temperature was found. After that, the average dry-bulb temperature was used to calculate the properties in Eq.(8) and the heat transfer coefficient. Finally, the air outlet dry-bulb temperature  $T_{a3}$  (Eq.(7)), humidity  $W_{a3}$  (humidity was determined by air dry- and wet-bulb temperature according to ASHRAE Handbook [29]), cooling efficiency (Eq.(10)) and pressure drop (Eq.(9)) were calculated.



Step 4, Step 1 and Step 2 were repeated using the new temperature  $T_{a3}$  and humidity  $W_{a3}$  calculated in Step 3. After calculations, a new air mass flow rate  $m_{a2}$  was obtained. The wetted-medium evaporative cooling was recalculated using the new air mass flow rate  $m_{a2}$  (repeating Step 3) and new values of cooling efficiency and pressure drop were found.

Step 5, it was then to make sure that the assumed cooling efficiency in Step 3 was consistent with that calculated in Step 4, and to check the consistency of pressure drop in Step 3 and Step 4. This was finished by a period of iteration of Step 4 with an increase in the initial cooling efficiency by an iteration variable in each iteration. After that, a closer air mass flow rate  $m_a$  could be found.

Step 6, the energy equations were balanced by a period of iteration. If the air mass flow rate  $m_a$  found in Step 5 could not satisfy the energy equations, the air temperature leaving the heat exchanger was reduced and Step 1-Step 5 were reiterated.

Finally, a value of air mass flow rate could be found that would satisfy both the energy and draft equations. Meanwhile, it was ensured that the assumed cooling efficiency in Step 3 was consistent with that calculated in Step 4, and the pressure drop in Step 3 approached well to that in Step 4.

Fig. 4 is the flow chart for the iteration loops described above.  $i$  is iteration variable and  $n$  is the judgement of termination. During simulation,  $i$  was taken as  $10^{-2}$  and  $n$  was taken as  $10^6$  at first. After  $|Q_1 - Q_2| < n$ ,  $i$  was reduced to  $10^{-4}$  and  $n$  was reduced to  $10^4$  to do more accurate iterations. Since there is no wetted-medium pre-cooling in use so far in NDDCTs, it was difficult to do a rigour comparison with the measured NDDCT performance. However, the MATLAB code of NDDCT without pre-cooling system was compared with the case study reported by Kroger [1] and found good agreement. This validated MATLAB code was then adapted to simulate the operation of the proposed tower with and without pre-cooling. The thermodynamic parameters were calculated according to references [1, 29]. The meteorological effects were considered according to Kroger's book [1]. The wetted medium performance was calculated according to our simplified model combined with A. Franco's correlations [6].

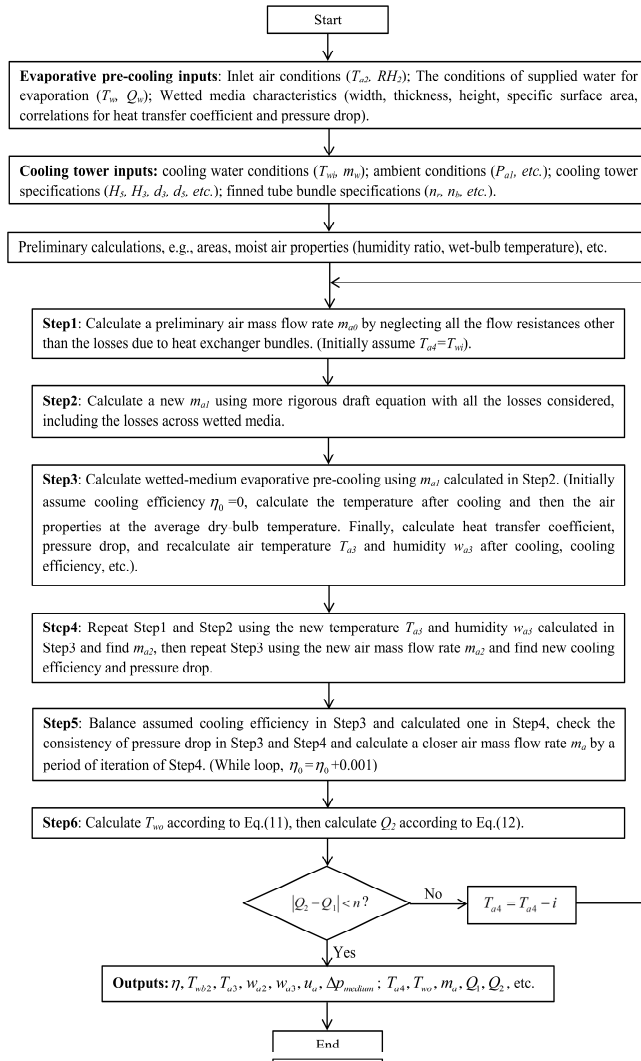


Fig. 3. Flow chart of the MATLAB code for the pre-cooled NDDCT model

## 4. Results and Discussions

The wetted medium used in the simulation was 100mm thick cellulose medium. The ambient temperature of 20°C was the design point of the proposed tower. All the results reported herein were from the numerical simulation described above. The wetted medium performance was coupled with the tower performance.

### 4.1 Wetted Medium Performance

The predicted performance of wetted media when placed in the form of a cylindrical shell around the tower inlet is reported in this section. The supplied water flow rates to the media in A. Franco's [6] tests didn't affect cooling efficiency and heat transfer coefficient as the flow rates could fully wet the media (fully wetted medium means there is no streaking and dry area in the medium) and were more than the amount of evaporated water [6, 30-32]. Therefore, the heat transfer coefficient is only presented at supply water flow rate of 0.128 l/s per m<sup>2</sup> air face area. The pressure drop is presented at two water flow rates as water flow rate affects pressure drop (see Eq.(9)).

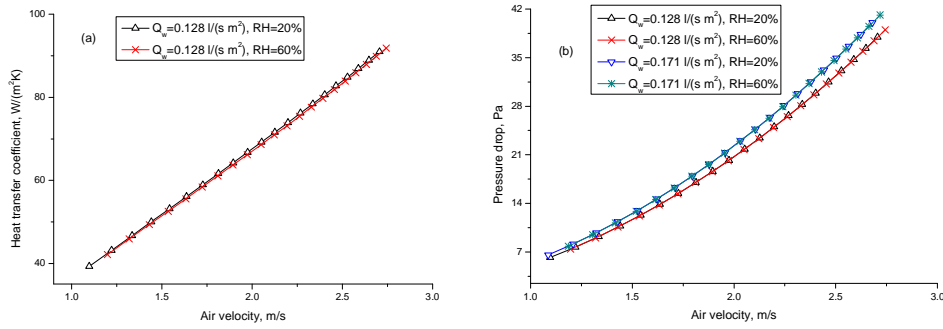


Fig. 4. (a) Heat transfer coefficient and (b) pressure drop of cellulose medium

For the studied cellulose medium, within the studied air velocity range, Fig. 4a shows that the heat transfer coefficient increases with the increase in air velocity, this is in agreement with C.M. Liao and R. Rawangkul [16, 33, 34] (see Eq.(8)). However, the heat transfer will not increase for no limit since the water may be carried away by air rather than evaporation at high air velocity, and the contact time between water and air in wetted media is decreased. The effect of relative humidity on heat transfer coefficient is negligible in Fig. 4a, which is because the effect of humidity on  $Nu$ ,  $Re$  and  $Pr$  in Eq.(8) is weak.

The pressure drop also increases with the air velocity increased as shown in Fig. 4b (see Eq.(9)), which is in accordance with literature [16, 33-37]. The effect of relative humidity on pressure drop is weak. Increasing the water flow rate supplied to the media, there is an increase in pressure drop for a given air velocity. Since the increase in water flow increases the sheet of water flowing over the inside transfer surface, and therefore decreasing the volume for air flow in the media, and as a result increases the pressure drop.

#### 4.2 Tower Performance

The pre-cooled NDDCT performance is reported in this section. The air mass flow rate and the heat rejection rate of NDDCTs are compared in Fig. 5 and Fig. 6.

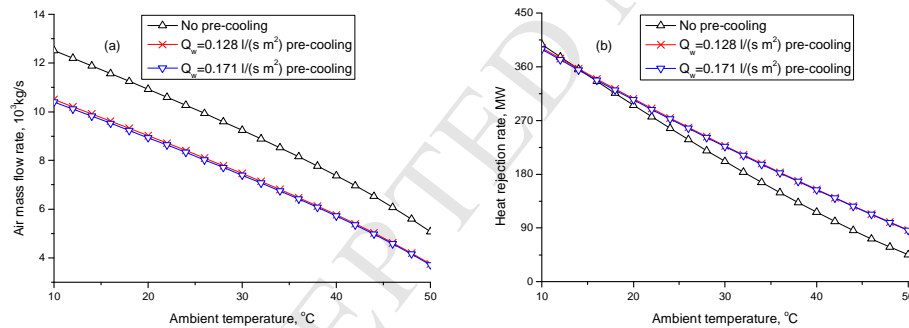


Fig. 5. The (a) air mass flow rate and (b) heat rejection rate of the NDDCTs (RH=20%)

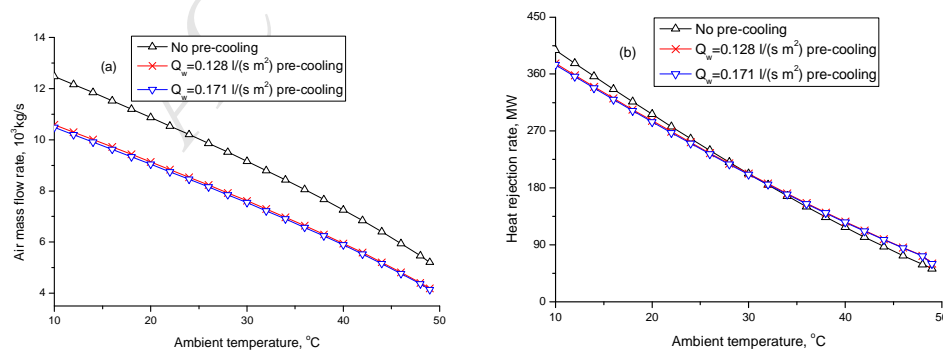


Fig. 6. The (a) air mass flow rate and (b) heat rejection rate of the NDDCTs (RH=60%)

The changes in air mass flow rate of the towers with, and without pre-cooling at relative humidity of 20% and 60% are depicted in Fig. 5a and Fig. 6a, respectively. The air mass flow rate decreases with the increase in ambient temperature, which is because the driving force (buoyancy, which is due to the air density difference resulting from the temperature difference between the tower inside and outside air, as Eq.(19)) is lower at higher ambient temperatures. This applies to the towers with or without pre-cooling. Fig. 5a and Fig. 6a also illustrate that the incorporation of pre-cooling into the proposed NDDCT, causes a further reduction in air mass flow rate due to the additional pressure drop associated with the media.

As can be seen from Fig. 5a and Fig. 6a, the effect of supplied water flow rate on air mass flow rate is negligible. This is due to two reasons: (1) both the heat transfer coefficient and cooling efficiency are insensitive to the supplied water flow rates as already stated in section 4.1; (2) the pressure drop increases slowly with increasing water flow rate as shown in Fig. 4b. The small difference in pressure drop caused by the changes in water flow is negligible when compared with other pressure drops encountered in the studied NDDCT (see Eq.(20) and Eq.(21)). These two reasons apply to the heat rejection rate as well, making it insensitive to the supplied water flow rates (as shown in Fig. 5b and Fig. 6b).

In terms of heat rejection, although pre-cooling decreases the inlet air temperature of the heat exchanger and thus improves heat rejection through Eq.(11), the additional pressure drop causes the drop in air mass flow rate and therefore impairs heat rejection. That is why heat rejection rate of the pre-cooled NDDCT can be either higher or lower than that of the tower without pre-cooling. This trend is very clear in Fig. 6b as the heat rejection rate of the pre-cooled NDDCT is lower at cool temperature but higher at hot temperature than that of the tower without pre-cooling. As evaporative cooling is more effective in hot and dry climates [6, 16], this means that pre-cooling would work better at higher ambient temperatures for a given humidity. This is demonstrated by the simulation results plotted in Fig. 5b and Fig. 6b as pre-cooling improves tower heat rejection at higher ambient temperatures. However, it is necessary to mention that since both the air mass flow rate and the temperature difference between the inlet air and inlet water of the heat exchanger decrease at higher ambient temperatures, the heat rejection of all the towers drops (as shown in Fig. 5b and Fig. 6b). There is a critical ambient temperature value below which pre-cooling does not help the NDDCT performance but hinders it. This critical temperature depends on the tower and heat exchanger geometry, medium type and thickness, air relative humidity. For the 120m height NDDCT considered in this study and for the 100mm thick cellulose medium at all the water flow rates, the critical temperatures are 14°C and 31°C at relative humidity of 20% and 60%, respectively (see Fig. 5b and Fig. 6b). Fig. 5b and Fig. 6b also demonstrate that NDDCT can benefit from wetted-medium pre-cooling when the ambient air is hot and dry (e.g., the tower heat rejection improvement goes up to 33% at ambient temperature of 40°C with 20% relative humidity), but the improvement declines quickly at increasing humidity (e.g., only 7% improvement at ambient temperature of 40°C with 60% relative humidity).

Comparing Fig. 5 and Fig. 6, one can find that the effect of relative humidity on air mass flow rate is weak. However, relative humidity affects the critical temperature to a large extent; the value of critical temperature is higher when the ambient humidity is higher. This is because relative humidity affects the air temperature to the heat exchanger through evaporative cooling and then the tower heat rejection through Eq.(11).

#### 4.3 Water Evaporation Rate

The evaporation rates at water flow rates of 0.128 and 0.171 l/s per m<sup>2</sup> air face area are illustrated in Fig. 7.

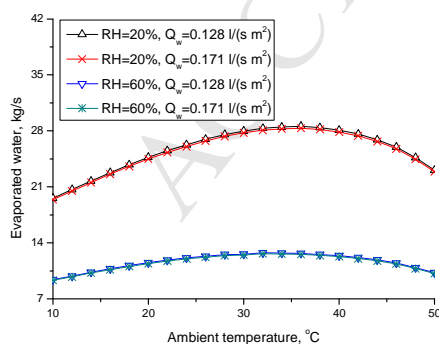


Fig. 7. Water evaporation rate of pre-cooling system

Fig. 7 reflects that the water evaporation rate, at increasing ambient temperature, experiences an increase and then a marginal decline. For a given humidity, higher ambient temperature is more beneficial for evaporative cooling, and thus larger humidity difference takes place. However, for NDDCT case, air flow is lower at higher

temperature as demonstrated in Fig. 5a and Fig. 6a. Since water evaporation rate is the combination of air mass flow rate and humidity difference (as shown in Eq.(1)), there is a trade-off between them. The evaporation rates peak at ambient temperatures of 36°C for 20% humidity and 32°C for 60% humidity at both water flow rates. Fig. 7 shows that the water evaporation rate is higher at lower humidity as evaporative cooling is more effective at hot and dry conditions. The effect of water flow on water evaporation is negligible.

The results presented above are based on ambient humidity of 20% and 60%. For real climatic conditions, the humidity may exceed this value, and the heat rejection rates will be lower than that in Fig. 5b and Fig. 6b. The average water consumption of pre-cooling system will depend on the ambient conditions, specifications of the cooling tower and type of wetted media. On a typical hot and dry day in Charleville, Australia, a 100m height NDDCT pre-cooled with CELdek7060, as reported by S. He [38], the day-average water consumption rate per MW heat rejection of the pre-cooled tower was approximately half of the wet cooling tower water consumption (The normal power output of the binary-cycle geothermal power plant was 29 MWe, and the pre-cooling system was turned on the whole day). This is a substantial benefit for plants in dry regions where wet cooling is infeasible.

## 5. Conclusions

The main conclusions are:

- The effect of supplied water flow rates on tower performance is negligible as long as the flow rates can fully wet the medium.
- Both the ambient temperature and humidity affect the tower performance.
- The water evaporation rate of pre-cooling is less than that of wet cooling tower.
- NDDCTs benefit from wetted-medium pre-cooling when ambient air is hot and dry, but the improvement declines quickly at increasing humidity. Care must be taken in designing pre-cooling of NDDCTs.

Wetted-medium pre-cooling is an important consideration for future EGS geothermal and concentrated solar thermal plants in Australia and the rest of the world, most of which are expected to be constructed in inland regions and dry climates.

## Acknowledgements

This research was performed as part of the Australian Solar Thermal Research Initiative (ASTRI), a project supported by Australian Government. The author, Suoying He, would also like to thank China Scholarship Council (CSC) for their financial support.

## References

- [1] D.G. Kroger, *Air-Cooled Heat Exchangers and Cooling Towers: Thermal-flow performance evaluation and design* Vol. 2, PennWell Corp., Tulsa, Oklahoma, USA, 2004.
- [2] PDHengineer, *Cooling Towers*, viewed: 15<sup>th</sup> June 2013, Retrieved from: [www.pdhengineer.com/courses/m/M-7002.pdf](http://www.pdhengineer.com/courses/m/M-7002.pdf).
- [3] D.G. Kroger, *Air-Cooled Heat Exchangers and Cooling Towers: Thermal-flow performance evaluation and design* Vol. 1, PennWell Corp., Tulsa, Oklahoma, USA, 2004.
- [4] A. Ashwood, D. Bharathan, *Hybrid Cooling Systems for Low-Temperature Geothermal Power Production*, Technical Report NREL/TP-5500-48765, Contract No. DE-AC36-08GO28308, U.S. Department of Energy, Colorado, USA, 2011, viewed: 16<sup>th</sup> June 2013, Retrieved from: [www.nrel.gov/docs/fy11osti/48765.pdf](http://www.nrel.gov/docs/fy11osti/48765.pdf).
- [5] C. Kutscher, D. Costenaro, *Assessment of Evaporative Cooling Enhancement Methods for Air-Cooled Geothermal Power Plants*, Paper presented to Geothermal Resources Council (GRC) Annual Meeting, Reno, Nevada, USA (22-25<sup>th</sup> Sep. 2002), pp. 1-9.
- [6] A. Franco, D.L. Valera, A. Madueno, A. Pena, *Influence of water and air flow on the performance of cellulose evaporative cooling pads used in Mediterranean greenhouse*, *Transactions of the ASABE* 53 (2010) 565-576.
- [7] A. Franco, D.L. Valera, A. Pena, A.M. Perez, *Aerodynamic analysis and CFD simulation of several cellulose evaporative cooling pads used in Mediterranean greenhouses*, *Computers and Electronics in Agriculture* 76 (2011) 218-230.
- [8] S. He, H. Gurgenci, Z. Guan, A. M. Alkhedhair, *Pre-cooling with Munters media to improve the performance of Natural Draft Dry Cooling Towers*, *Applied Thermal Engineering* 53 (2013) 67-77.
- [9] Australasian Agricultural Services Pty Ltd., 2002, viewed: 09<sup>th</sup> July 2013, Retrieved from: [www.ausagservices.com.au/deals/aug12.html](http://www.ausagservices.com.au/deals/aug12.html).
- [10] J.R. Watt, W.K. Brown, *Evaporative Air Conditioning Handbook*, third ed., Fairmont Press, Inc., Lilburn, Georgia, USA, 1997.
- [11] M. Lucas, P.J. Martinez, J. Ruiz, A.S. Kaiser, A. Viedma, B. Zamora, *The dry and adiabatic fluid cooler as an alternative to cooling towers: an experimental view*, *Proceedings of the 15<sup>th</sup> IAHR Cooling Tower and Air-cooled Heat Exchanger Conference & 2011 Annual Symposium of Industrial Cooling Tower Study Committee of CSEE Thermal Power Chapter*, Beijing, China (23-26<sup>th</sup> Oct. 2011), pp. 364-372.
- [12] A.U. Dzivama, U.B. Bindir, F.O. Aboaba, *Evaluation of pad materials in construction of active evaporative cooler for storage of fruits and vegetables in arid environment*, *Agricultural Mechanization in Asia, Africa and Latin America* 30 (1999) 51-55.
- [13] E.E. Anyanwu, *Design and measured performance of a porous evaporative cooler for preservation of fruits and vegetables*, *Energy Conversion and Management* 45 (2004) 2187-2195.
- [14] USGR, *Evaporative cooling pads and cooling ventilation system from USGR*, viewed: 06<sup>th</sup> July 2013, Retrieved from: [www.usgr.com/cooling-pads/index.php](http://www.usgr.com/cooling-pads/index.php).

- [15] C. Lertsatitthanakorn, S. Rerngwongwitaya, S. Soponronnarit, Field Experiments and Economic Evaluation of an Evaporative Cooling System in a Silkworm Rearing House, *Biosystems Engineering* 93 (2006) 213-219.
- [16] C.M. Liao, K.H. Chiu, Wind tunnel modeling the system performance of alternative evaporative cooling pads in Taiwan region, *Building and Environment* 37 (2002) 177-187.
- [17] R. Hosseini, A. Beshkani, M. Soltani, Performance improvement of gas turbines of Fars (Iran) combined cycle power plant by intake air cooling using a media evaporative cooler, *Energy Conversion and Management* 48 (2007) 1055-1064.
- [18] H.R. Goshayshi, J.F. Missenden, R. Tozer, Cooling tower-an energy conservation resource, *Applied Thermal Engineering* 19 (1999) 1223-1235.
- [19] E. Elsarrag, Experimental study and predictions of an inclined draft ceramic tile packing cooling tower, *Energy Conversion and Management* 47 (2006) 2034-2043.
- [20] J.C. Kloppers, A critical evaluation and refinement of the performance prediction of wet cooling towers, PhD thesis, University of Stellenbosch, Stellenbosch, South Africa, 2003.
- [21] Munters, Munters products handbook, viewed: 08<sup>th</sup> July 2013, Retrieved from: [www.munters.com/en/Global/](http://www.munters.com/en/Global/).
- [22] S. Wasim, B. Frank, L. Ming, Technical Background Research on Evaporative Air Conditioners and Feasibility of Rating Their Water Consumption, Contract No. Canberra ACT 2601, Institute for Sustainable Systems and Technologies, The University of South Australia, South Australia, Australia, 2009, viewed: 01<sup>st</sup> July 2013, Retrieved from: [www.waterrating.gov.au/sites/www.waterrating.gov.au/files/publications/2009/09/107/evaporative-air-conditioners.pdf](http://www.waterrating.gov.au/sites/www.waterrating.gov.au/files/publications/2009/09/107/evaporative-air-conditioners.pdf).
- [23] R.A. Bucklin, J.D. Leary, D.B. McConnell, E.G. Wilkerson, Fan and Pad Greenhouse Evaporative Cooling Systems, 1993, viewed: 09<sup>th</sup> July 2013, Retrieved from: [www.edis.ifas.ufl.edu/ae069](http://www.edis.ifas.ufl.edu/ae069).
- [24] J.M. Wu, X. Huang, H. Zhang, Theoretical analysis on heat and mass transfer in a direct evaporative cooler, *Applied Thermal Engineering* 29 (2009) 980-984.
- [25] S.E. Haaland, Simple and explicit formulas for the friction factor in turbulent pipe flow, *Journal of Fluids Engineering* 105 (1983) 89-90.
- [26] W. Roetzel, J. Neubert, Calculation of mean temperature difference in air-cooled cross-flow heat exchangers, *Journal of Heat Transfer* 101 (1979) 511-513.
- [27] V. Gnielinski, New equations for heat and mass transfer in turbulent pipe and channel flow, *International Chemical Engineering* 16 (1976) 359-368.
- [28] H. Rouse, *Elementary Mechanics of Fluids*, John Wiley & Sons, Inc., New York, USA, 1946.
- [29] ASHRAE, *ASHRAE Handbook-Fundamentals*, I-P ed., American Society of Heating, Refrigerating and Air-Conditioning Engineers, Inc., Atlanta, USA, 2009.
- [30] R.D. Trumbull, J.L. Koon, C.A. Flood, Potential for use of evaporative cooling systems, Paper presented to summer meeting of American society of agricultural engineers, San Luis Obispo, California, USA (29<sup>th</sup> June-2<sup>nd</sup> July, 1986), pp. 1-14.
- [31] Q. Zhang, P. Chen, Heat and mass transfer performance of a domestic product of sprayed corrugated cellulose media, *Journal of Tongji University* 23 (1995) 648-653.
- [32] Z. Wei, S. Geng, Experimental Research on Direct Evaporative Cooling of Organic Padding, *Contamination Control and Air-Conditioning Technology* 1 (2009) 22-26.
- [33] C.M. Liao, S. Singh, T.S. Wang, Characterizing the performance of alternative evaporative cooling pad media in thermal environmental control applications, *Journal of Environmental Science and Health, Part A* 33 (1998) 1391-1417.
- [34] R. Rawangkul, J. Khedari, J. Hirunlabh, B. Zeghamati, Performance analysis of a new suitable evaporative cooling pad made from coconut coir, *International Journal of Sustainable Engineering* 1 (2008) 117-131.
- [35] R.W. Koca, W.C. Hughes, L.L. Christianson, Evaporative cooling pads: test procedure and evaluation, *Applied Engineering in Agriculture* 7 (1991) 485-490.
- [36] A. Malli, H.R. Seyf, M. Layeghi, S. Sharifian, H. Behraves, Investigating the performance of cellulosic evaporative cooling pads, *Energy Conversion and Management* 52 (2011) 2598-2603.
- [37] M. Barzegar, M. Layeghi, G. Ebrahimi, Y. Hamzeh, M. Khorasani, Experimental evaluation of the performances of cellulosic pads made out of Kraft and NSSC corrugated papers as evaporative media, *Energy Conversion and Management* 54 (2012) 24-29.
- [38] S. He, H. Gurgenci, Z. Guan, Y. Lu, Investigation of Pre-Cooling with Munters Media for Air-Cooled Geothermal Power Plants Performance Enhancement, *Proceedings of the 2012 Australian Geothermal Energy Conference*, Sydney, Australia (13-16<sup>th</sup> Nov. 2012), pp. 81-85.

**Figure Captions**

- Fig. 1. NDDCT pre-cooled with cellulose media (not to scale)
- Fig. 2. Transfer process of evaporative cooling system and a control volume
- Fig. 3. Flow chart of the MATLAB code for the pre-cooled NDDCT model
- Fig. 4. (a) Heat transfer coefficient and (b) pressure drop of cellulose medium
- Fig. 5. The (a) air mass flow rate and (b) heat rejection rate of the NDDCTs (RH=20%)
- Fig. 6. The (a) air mass flow rate and (b) heat rejection rate of the NDDCTs (RH=60%)
- Fig. 7. Water evaporation rate of pre-cooling system

**Highlights**

- We develop a model to simulate wetted media and natural draft dry cooling tower.
- We examine the influence of ambient conditions and water flow on tower performance.
- The effect of water flow on tower performance is negligible.
- Dry cooling tower can benefit from pre-cooling when the ambient air is hot and dry.
- The water evaporation rate of pre-cooling is less than wet cooling tower.